Erschienen in: Journal of Magnetism and Magnetic Materials ; 469 (2019). - S. 217-223.
https://dx.doi.org/10.1016/j.jmmm.2018.08.034

Spin-lattice relaxation beyond Gilbert damping

Matthias Aßmann*, Ulrich Nowak

Fachbereich Physik, Universität Konstanz, D-78457 Konstanz, Germany

ARTICLE INFO

Keywords:
Magnetic damping
Spin-lattice coupling
Classical spin models

ABSTRACT

A combined dynamics for the spin and lattice degrees of freedom is proposed. For that we couple a Heisenberg spin Hamiltonian via a distance dependent exchange integral and an anisotropic correction to the lattice, where the latter is formed by a harmonic potential. With these extensions the transfer of energy as well as angular momentum between lattice and spins is possible. We test this model successfully by reproducing the Einstein-De Haas effect for a free cluster. On the other hand we find severe differences of the temperature dependent demagnetization dynamics of the new approach as compared to the well-established magnetization dynamics covered by Gilbert damping.

1. Introduction

Since the discovery of ultrafast magnetization processes [1] the flow of energy and angular momentum between spin, electron, and phonon degrees of freedom, their underlying microscopic mechanisms and associated time scales move in the focus of current research. Experiments lead to the conclusion [2] that efficient channels exist for the spin angular moment to dissipate into the lattice. However, this phenomenon and its underlying mechanisms are still controversially discussed [3–7].

Improved imaging techniques allow to track even atomic movement on ultrashort time scales during magnetization processes[8–10]. These experiments are available now to examine the mechanisms of spin-lattice coupling fundamentally, fostering an interest in theory and modeling of these interactions. Furthermore, spin-lattice coupling is very important in the field of spin-caloritronic transport in insulators, where the lattice and spin subsystem are on different temperatures, leading to a flow of energy and angular momentum between both systems [11].

The most common way for modeling dissipative magnetization dynamics is to assume one single phenomenological damping parameter which represents the coupling of the magnetic systems to a heat-bath. This parameter is used in the equation of motion, normally the Landau-Lifshitz-Gilbert equation (LLG) [12,13]. This approach completely neglects any subtleties coming from the interactions of the spins with the electrons and the lattice, respectively. The challenge in this context is to explain the damping processes on a microscopic basis. While the coupling to the electronic reservoir [14–17] and the intrinsic magnon scattering processes[18] have been discussed before, atomistic models which determine the coupling to the lattice directly are still rare [19–23]. The reason for that is the enormous effort in *ab initio* calculations to treat the spin-orbit interaction, which allows for the necessary transfer of spin angular momentum into the lattice. As one needs the full electronic structure of the material, the numerical complexity restricts the size of the samples to a few atoms. Otherwise one has to assume perfect lattice symmetries and cannot take distortions through, e.g., phonons into account.

In this work, we present a phenomenological spin-lattice coupling term, which arises from anisotropic correction to the Heisenberg exchange. With this Hamiltonian we perform simulation for the dynamics of the spins and the lattice and treat all degrees of freedom on equal footing. This combined molecular dynamics with spin dynamics (MD-SD) [22] approach obeys the conservation laws for total energy and total angular momentum strictly. We also present a possible parametrization that can be used to relate our model parameters to known material parameters.

2. Spin-lattice coupling

For the coupling of the lattice with the magnetic degrees of freedom this paper follows a microscopic path for which we use an atomistic Hamiltonian based on a Heisenberg model with localised magnetic moments $\mathbf{S}_i = \boldsymbol{\mu}_i/\mu_s$, where $\boldsymbol{\mu}_i$ is the magnetic moment of the atom i at position $\mathbf{r}_i$ and μ_s its magnitude. The localised moments are interacting via distance dependent exchange integrals approximated by a steady exchange function $J(r_{ij})$. Furthermore, an anisotropic part for the exchange is considered by an additional term that represents second order corrections [27] caused by Spin-orbit interaction. The total magnetic exchange is then assumed as

* Corresponding author.
E-mail address: matthias.assmann@uni-konstanz.de (M. Aßmann).

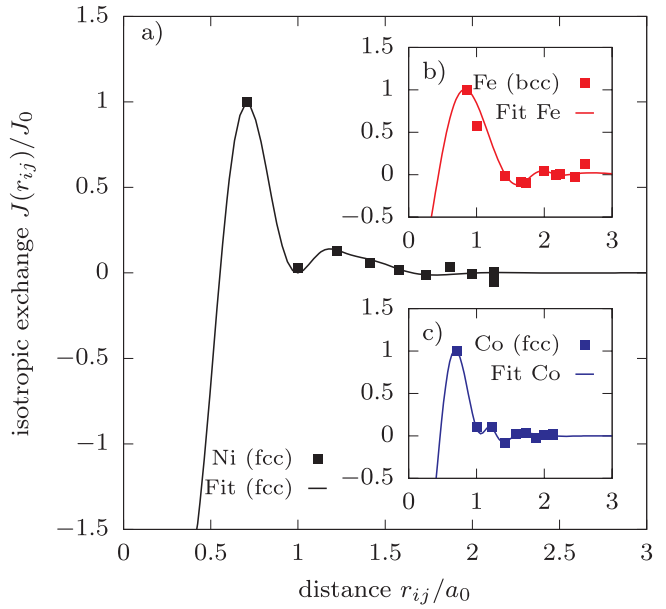

Fig. 1. Isotropic exchange Interaction between pairs of atoms for different ferromagnetic materials. All data are taken from [29]. Solid lines are the fits following Eq. (2).

$$\mathscr{H}_{\text{exc}} = \underbrace{-\sum_{\langle i,j\rangle} J(r_{ij})(\mathbf{S}_i\cdot\mathbf{S}_j)}_{\mathscr{H}_{\text{iso}}} + \underbrace{\lambda C \sum_{\langle i,j\rangle} \frac{(\mathbf{S}_i\cdot\mathbf{r}_{ij})(\mathbf{r}_{ij}\cdot\mathbf{S}_j)}{r_{ij}^6}}_{\mathscr{H}_{\text{anis}}}, \tag{1}$$

where $C = J_0\left(\frac{\mu_0\mu_s^2}{J_0}\right)^{4/3}$. Both terms are necessary, since the scalar isotropic exchange defines the ferromagnetic ground state, but allows only the transfer of energy to the lattice and vice versa, while the anisotropic terms makes the transfer of angular momentum between magnetic system and lattice possible. Because both terms depend on the spin-configuration as well as the lattice coordiates, the lattice and the magnetic system can directly interact with each other without any restrictions due to angular momentum conservation.

The isotropic exchange function $J(r_{ij})$ is material specific and difficult to obtain. Different attempts to find a suitable form for $J(r_{ij})$ phenomenologically were made [28,22]. For this work we use a function of the form

$$J(r_{ij}) \tag{2}$$

which can be well fitted to ab initio data[29]. For the ferromagnetic materials Fe, Co, Ni the behavior of the exchange function is shown in Fig. 1. The function (2) catches most of the features of the ab initio data for the exchange coupling. For distances smaller than the first neighbors the coupling must become antiferromagnetic due to Pauli's principle. The coupling of the first neighbors can be well approximated as well as the decay for large distances. The cos-part leads to oscillations which are well known in metals as RKKY-exchange [30–32].

The influence of the spin-orbit coupling, which causes the necessary anisotropy for the angular momentum transfer between magnetic and lattice system, is approximately treated by $\mathscr{H}_{\text{anis}}$ in this work. Since it has never been calculated reliably with ab initio methods, experimental data is used for its parametrization, which are analyzed in the context of the theory of magneto-elasticity. In this framework the continuous magnetization field **M** is coupled in second order to the elastic strain tensor **e**, which describes the lattice system. For the coupling in cubic lattice systems one gets the following terms in the free energy [20,24,25],

$$U_{\text{Mag-Ela}} = \frac{B_1}{M_0^2}\sum_i M_i^2 e_{ii} + \frac{B_2}{M_0^2}\sum_i\sum_{j,j\neq i} M_i M_j e_{ij} + \frac{A_1}{M_0^2}\sum_i\sum_j\sum_{l,l\neq j}\frac{\partial M_i}{\partial x_j}\frac{\partial M_j}{\partial x_l}e_{jl} + \frac{A_2}{M_0^2}\sum_i\sum_j\left(\frac{\partial M_i}{\partial x_j}\right)^2 e_{jj}. \tag{3}$$

Here the first two parts come from anisotropic interactions, like the dipole-dipole interaction or the spin-orbit coupling, while the last two terms arise from the isotropic exchange interaction. The constants B_1 and B_2 characterize the strength of anisotropic interactions which are responsible for the transfer of angular momentum. The arising equations of motion can be used to study the dynamics of magneto-elastic excitations[26]. In the following only the energy scale of the experimental accesible constants B_1 and B_1 are used for the further microscopic calculations based on Eq. (1).

The anisotropic part in Eq. (1) is parametrized by λ in a way, that its value reproduces the ratio of anisotropic to isotropic energies in the magneto-elastic expression of Eq. (3) for the microscopic terms in Eq. (1), leading to

$$\frac{\lambda\mathscr{H}_{\text{anis}}}{\mathscr{H}_{\text{iso}}} \approx \frac{(|B_1| + |B_2|)a_0^3}{K_B\, T_C}, \tag{4}$$

where the total isotropic exchange is parametrized via the Curie temperature T_C of the material. Here, a_0 is the lattice constant of the specific material. Consequently, it is possible to find suitable parameters to model different materials based on ab initio data and their magneto-elastic constants. In Table 1 the resulting parameters are summarized for common ferromagnetic materials. Furthermore, the used fitting parameters for the isotropic exchange functions $J(r_{ij})$ are given.

3. Model and equations of motion

To complete the overall model, the total Hamiltonian $\mathscr{H}_{\text{total}}$ consists of two parts, namely the magnetic part $\mathscr{H}_{\text{mag}}$ and the lattice part $\mathscr{H}_{\text{lat}}$. The magnetic part includes besides the exchange interaction presented in Eq. (1) the Zeeman-energy in an external field $\mathbf{B_0}$,

$$\mathscr{H}_{\text{mag}} = \mathscr{H}_{\text{exc}} \underbrace{-\mu_s \mathbf{B}_0 \sum_i \mathbf{S}_i}_{\mathscr{H}_{\text{zeeman}}}. \tag{5}$$

Table 1
Parametrization for Fe, Co, Ni. The magneto-elastic constants and the values for the Young modulus of Fe, Co, Ni are taken from Ref. [33], the other material parameters from Ref. [34]. The atomic masses are given in unified atomic mass units (u). The fitting parameters for the exchange function are listed in the last part.

	Fe (bcc)	Co (fcc)	Ni (fcc)
$\mathscr{Y}$ (GPa)	131	114	133
V_0 (10^{-20} J)	2.416	1.588	1.864
a_0 (Å)	2.87	3.54	3.52
m_i (u)	55.85	58.93	58.71
Θ_D (K)	420	385	375
μ_s (μ_B)	2.2	1.6	0.6
T_C (K)	1043	1390	650
J_0 (10^{-20}J)	0.538	0.435	0.145
B_1 (MJ m^{-3})	−3.43	−9.2	9.38
B_2 (MJ m^{-3})	7.83	7.7	10
$(\|B_1\| + \|B_2\|)a_0^3/K_B T_C$	0.018	0.039	0.094
d_1 (a_0)	0.93	0.74	0.735
d_2 (a_0)	1.90	1.195	1.10
ω ($1/a_0$)	3.2	5.68	8.5
ξ ($1/a_0$)	2.4	3.95	4.7
γ ($1/a_0^2$)	15.0	53.0	35.0
C_1 (J_0)	1.89	1.92	1.93
C_2 (J_0)	0.2	0.34	0.39

The lattice part $\mathscr{H}_{\text{lat}}$ includes the classical kinetic and potential energies,

$$\mathscr{H}_{\text{lat}} = \sum_i \frac{\mathbf{p}_i^2}{2m_i} + V_{\text{harm}}. \tag{6}$$

The potential leads to lattice formation. It is assumed simply harmonic

$$V_{\text{harm}} = V_0 \sum_{\langle i,j \rangle} (r_{ij} - \sigma_{ij})^2, \tag{7}$$

where σ_{ij} is the equilibrium distance for the considered atom pair. Here, all atom pairs up to a distance of $2a_0$ are considered. With the initialization of the set of σ_{ij} the lattice structure is clearly defined as the atoms can only move around their equilibrium positions.

The reason for choosing a harmonic potential is its simplicity and the reduced numerically effort. The harmonic potential is certainly a good approximation for a temperature regime where the amplitudes of the atomic motion is rather small. At the same time, going beyond nearest neighbor interaction, the lattice becomes stable even under torsional movement, a property that is otherwise hard to achieve with a pair-potential. For studies where structural changes play a role the use of more complex many-body potentials would be necessary. For temperatures above the Debye temperature Θ_D the approximation becomes less appropriate.

To parametrize the potential from known elastic properties we consider the Young modulus $\mathscr{Y}$ of the material and estimate the potential strength via

$$V_0 \approx \frac{\mathscr{Y} a_0^3}{2N}, \tag{8}$$

where N is the total number of neighbors for which the interactions are calculated. This approach leads to a potential which reproduces the interatomic forces of the material in the linear regime. The lattice model is not able to reproduce elastic anistropies or the correct thermal expansion of the lattice. As this work lies a special focus on the influence of the dynamic lattice on the magnetic system, we consider this shortcomings as acceptable. For the three ferromagnetic elements Fe, Co and Ni the corresponding numbers are given in Table 1. The total Hamiltonian is the sum of all parts,

$$\mathscr{H}_{\text{total}} = \mathscr{H}_{\text{mag}} + \mathscr{H}_{\text{lat}} = \underbrace{-\sum_{\langle i,j \rangle} J(r_{ij})(\mathbf{S}_i \cdot \mathbf{S}_j)}_{\mathscr{H}_{\text{iso}}} + \underbrace{\lambda C \sum_{\langle i,j \rangle} \frac{(\mathbf{S}_i \cdot \mathbf{r}_{ij})(\mathbf{r}_{ij} \cdot \mathbf{S}_j)}{r_{ij}^6}}_{\mathscr{H}_{\text{anis}}}$$
$$\underbrace{-\mu_s \mathbf{B}_0 \sum_i \mathbf{S}_i}_{\mathscr{H}_{\text{zeeman}}} + \underbrace{\sum_i \frac{\mathbf{p}_i^2}{2m_i}}_{\mathscr{H}_{\text{kin}}} + \underbrace{V_0 \sum_{\langle i,j \rangle} (r_{ij} - \sigma_{ij})^2}_{\mathscr{H}_{\text{harm}}} \tag{9}$$

Now the equations of motion for all degrees of freedom $\mathbf{p}_i$, $\mathbf{r}_i$ and $\mathbf{S}_i$ can be derived directly via

$$\begin{aligned} \dot{\mathbf{r}}_i &= \frac{\partial \mathscr{H}_{\text{total}}}{\partial \mathbf{p}_i} \\ \dot{\mathbf{p}}_i &= -\frac{\partial \mathscr{H}_{\text{total}}}{\partial \mathbf{r}_i} \\ \dot{\mathbf{S}}_i &= \{\mathbf{S}_i, \mathscr{H}_{\text{total}}\}. \end{aligned} \tag{10}$$

The classical evaluation of the Poisson-brackets for the spin leads to the torque equation[35]

$$\dot{\mathbf{S}}_i = -\frac{\gamma}{\mu_s} \mathbf{S}_i \times \mathbf{H}_i^{\text{eff}}, \tag{11}$$

where the effective field is give by

$$\mathbf{H}_i^{\text{eff}} = -\frac{\delta \mathscr{H}}{\delta \mathbf{S}_i}. \tag{12}$$

The most common approach to describe spin dynamics rests on the Landau-Lifshitz-Gilbert equation which neglects the motion of the atoms and extends the equation of motion for the spins above with a phenomenological damping term, characterized by damping constant α_{tot}, which also renormalizes the precession frequency,

$$\dot{\mathbf{S}}_i = -\frac{\gamma}{(1+\alpha_{\text{tot}}^2)\mu_s} \mathbf{S}_i \times \mathbf{H}_i^{\text{eff}} - \frac{\gamma \alpha_{\text{tot}}}{(1+\alpha_{\text{tot}}^2)\mu_s} \mathbf{S}_i \times (\mathbf{S}_i \times \mathbf{H}_i^{\text{eff}}). \tag{13}$$

In Eq. (13) γ is the gyromagnetic ratio for the chosen material. In this work the value for the free electron[36] $\gamma = 1.760859708 \times 10^{11}$ rad/sT is used. In the following, the dynamics obtained by the LLG equation is only used for comparison to the MD-SD approach using the equations of motion (10).

Finally, we define the angular momentum of the lattice via

$$\mathbf{L}_{\text{lat}} = \sum_i \mathbf{L}_i = \sum_i \mathbf{r}_i \times \mathbf{p}_i, \tag{14}$$

as the simulations perform classical dynamics.

4. Algorithm

To follow the flow of angular momentum it is necessary to use a symplectic algorithm, which treats all degrees of freedom equally. Different schemes have been developed, based on the Liouville formalism [37] and Suzuki-Trotter decompositions [38], which are able to handle the problem. In this paper the same decomposition as in Ref. [35] is used. The propagation of the spin system is described in Ref. [39]. The operators for position and momentum lead to a shift in phase space, as described in Ref. [37]. The algorithm is able to keep the total energy and phase space volume constant over the required timescales of several nanoseconds. We perform our simulations in the microcanonical ensemble since keeping the system at constant temperature would require the use of a thermostat, where most integration schemes are problematic regarding the angular momentum conservation. To define a temperature we use the equipartition theorem, where the temperature of whole system is defined through its total inner energy [37]. Starting from the inner energies of the parts one obtains

$$\underbrace{\left\langle \sum_i \frac{\mathbf{p}_i^2}{2m_i} \right\rangle}_{=3/2K_BT} + \underbrace{\langle V_{\text{harm}} \rangle}_{=3/2K_BT} + \underbrace{\langle \mathscr{H}_{\text{mag}} \rangle}_{=2/2K_BT} = 4K_BT \tag{15}$$

For the magnetic system the spin-wave approximation [40] for lower temperatures is used to approximate the heat capacity of the magnetic system. Furthermore in Eq. (15) only excitations from the magnetic ground state are taken into account, therefore one has to substract the ground-state energy U_{mag}^0. The system temperature is then calculated by

$$T_{\text{Sys}} = \frac{\langle \mathscr{H}_{\text{Lat}} \rangle + (\langle \mathscr{H}_{\text{mag}} \rangle - U_{\text{mag}}^0)}{4K_B}. \tag{16}$$

This formula is only valid after some equilibration time.

5. Results

5.1. Einstein-de Haas effect

As a first scenario we reproduce the Einstein-de Haas Effect [41] for a free magnetic particle. Here, the conservation laws for energy and angular momentum play a crucial role.We start our simulation with an almost homogeneously magnetized sample in an external field which points in the opposite direction. While the magnetization aligns with the external field angular momentum is transferred from the spin system into the lattice, so that the sample will begin to rotate. This effect relies on the conservation of total angular momentum. In these simulations we use a particle of cubic shape with an fcc lattice structure where the edge size is 6 atoms, corresponding to 666 atomic spins in total, with the parameters of Cobalt (see Table 1). As mentioned before, the simulation uses open boundary conditions to enable the conservation of total angular momentum.

To match the respective lattice temperature the positions of the atoms are initialized slightly off their equilibrium position, such that the resulting lattice temperature after equilibration is about 300 K. The

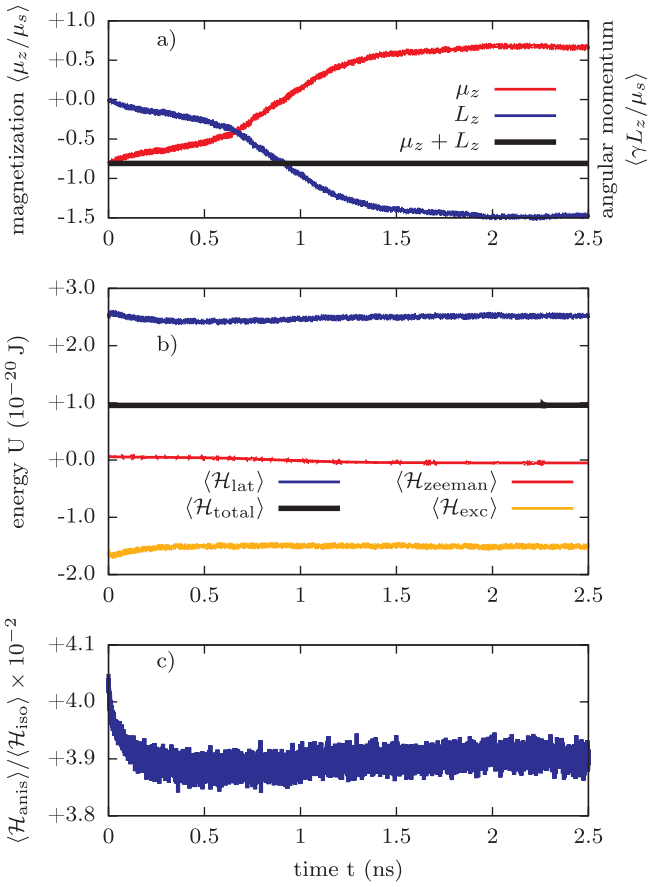

Fig. 2. a) z-components of reduced magnetization and angular momentum of the lattice versus time. The external field reverses the magnetization and the angular momentum flows from the spin system into the lattice. b) Different energy contributions versus time: first the energy mismatch of spin and lattice system equilibrates, then the rotation of the sample due to the angular momentum transfer increases the lattice energy slightly while the Zeeman energy shrinks. c) The ratio of anisotropic and isotropic exchange energy remains nearly constant during the switching process.

atoms are placed randomly within spheres with an adjusted radius. A Boltzmann distribution of the lattice momenta is then established within several picoseconds. Then an external field of 50 T in z-direction is applied. The spins are all aligned almost antiparallel to the field, so that a magnetization of $0.8\mu_s$ per atom is achieved. The sample magnetization is not exactly antiparallel to the external field to avoid a metastable state. The final results for the dynamics are obtained by averaging over 20 independent simulation runs, where the starting configuration of the initial atom positions is varied.

In Fig. 2a) the dynamic behavior of the z-components of the magnetization and of the lattice angular momentum is shown. One can see that the magnetization switches, finally pointing in field direction, while the spin angular momentum flows into the lattice. The z-component of the total angular momentum (spin plus lattice) remains constant. This flow of angular momentum leads to a rotation of the sample around its z-axis — the Einstein-de Haas effect. The external field breaks the rotation symmetry of x- and y-components, therefore these components of the total angular momentum are not conserved.

In Fig. 2b) the different parts of the energy are plotted versus time. The thermalization of the lattice degrees of freedom is nearly instantaneous. The slight mismatch between spin energy and lattice energy vanishes also after 300ps. The switching process of the magnetization takes longer and starts some time later. The induced rotation of the sample leads to a small increase of the lattice energy but also to a decrease of Zeeman energy. The total energy of the system is conserved as our model obeys all conservation laws.

In Fig. 2 c) the ratio between the anisotropic and the isotropic part of the exchange energy is shown. As the lattice is randomly disordered the ratio is in the beginning slightly higher, but converges to an equilibrium value while the lattice and spin degrees of freedom equilibrate. Then the ratio remains nearly constant and small during the whole switching process, so that it is justified to consider the coupling $\mathscr{H}_{\rm anis}$ as a small correction.

5.2. *Thermal demagnetization*

To gain a better understanding for the thermal non-equilibrium processes in magnetic materials the relaxation of lattice excitations and the resulting magnetic behavior is simulated. At the same time this procedure tests the resulting equilibrium magnetization for different lattice temperatures and the dynamics can be compared to the more established way of performing magnetization dynamics calculations at elevated temperatures within the framework of the stochastic LLG equation [42].

In a first step we vary the initial energy deposed in the lattice and determine the resulting saturation magnetization after the relaxation process. This approach is similar to the way the spin-lattice relaxation time is determined in Ref. [43]. To omit rotations of the sample the bottom layer is not integrated in time. This artificial residual magnetization is subtracted in the high temperature regime.

The results are shown in Fig. 3a). In the low temperature regime the residual magnetization drops nearly linear while it decays faster near the critical point. The model displays a magnetic phase transition. A small non-vanishing magnetization above the Curie-temperature is due to the finite size effect, an effect which is even increased by the open boundary conditions which are used in the simulations. Most importantly, the equilibrium properties agree well in the low temperature regime with simulations of the stochastic LLG equation which were also performed for the spin part of the model. In the high temperature regime the LLG simulations show more finite size effects as the phase space in the pure spin-dynamics is smaller.

Fig. 3b) illustrates the dynamics of the demagnetization process. The sigmoid shape differs clearly from the usual expectations, which would be an exponential behavior [44,45], and is analyzed in detail below. For increasing temperature the dynamics become faster, because the energy difference between lattice and magnetic system increases which leads to a stronger energy flow. There is a striking difference to the dynamic produced by the Landau-Lifshitz Gilbert equation as shown in 3 c), where the magnetization decays always nearly exponential. Only around the Curie temperature a deviation from that behavior due to a critical slowing down can be observed. In the MD-SD approach the dynamics is more complex, since spins as well as lattice contribute to each others equilibration mutually. Another important point is that this behavior seems to be more prominent in the regime of lower temperatures. So even in situations where both systems are energetically closer to each other, the energy transfer from the lattice into the magnetic system does not lead to a simple exponential decay and goes therefore beyond the description of the Landau-Lifshitz Gilbert equation.

To analyze the relaxation processes of the MD-SD approach quantitatively we chose a logistic approach for the inner energies $U_x = \langle \mathscr{H}_x \rangle$, namely

$$\begin{aligned} \frac{dU_{\rm lat}}{dt} &= \eta U_{\rm lat}(t)[\Delta U_0 - U_{\rm lat}(t)] \\ \frac{dU_{\rm mag}}{dt} &= -\eta U_{\rm mag}(t)[\Delta U_0 - U_{\rm mag}(t)]. \end{aligned} \tag{17}$$

The reason for choosing this ansatz is that in the beginning the lattice distortions have to create magnonic excitations to interact further. With increasing magnon population the dynamics become faster. In the end the amount of energy one can store in the magnetic system is limited,

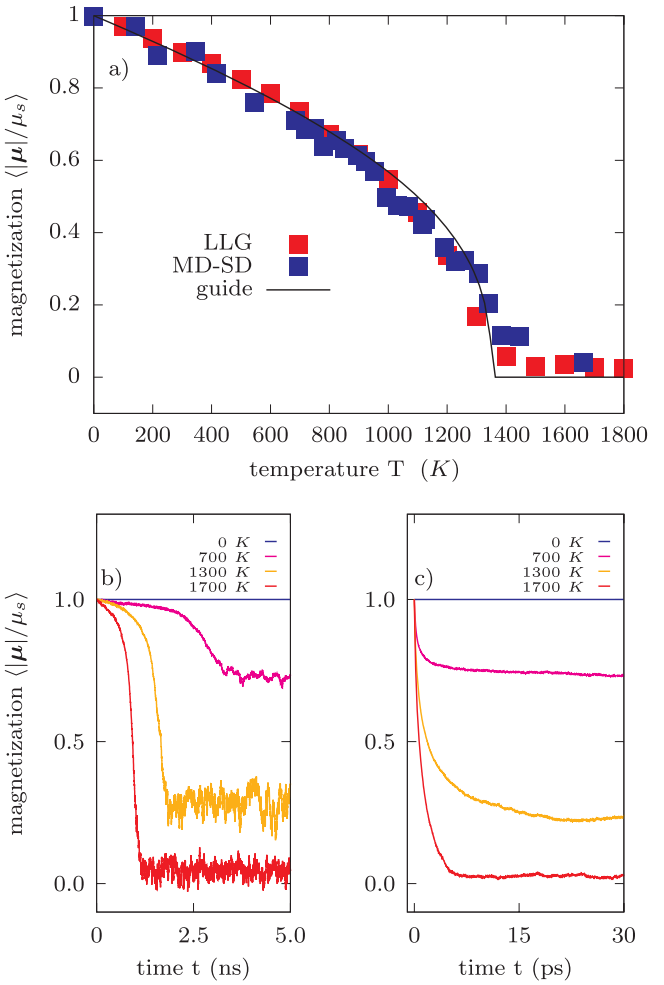

Fig. 3. Magnetization of a cobalt cluster. In a) the temperature dependence of MD-SD and LLG simulations is compared and agreement if found. The experimental Curie temperature of Cobalt is 1390 K, which can be approximately reproduced. b) Relaxation of the magnetization within the MD-SD approach. The magnetization decays non-exponential. c) Comparison to the LLG dynamics with damping constant $\alpha = 0.005$ and stochastic thermostat [42]. As one can see the relaxation, which is driven by the lattice is much slower. Even for high temperatures reaching equilibrium takes nearly two order of magnitudes longer.

therefore the inner energy has an upper border. After complete demagnetization only high frequency magnon modes are able to take further energy, but this processes become less likely with increasing energy flow. The Eqs. (17) have solutions of the form

$$U_{\text{lat}} = U_0^{\text{lat}} - \frac{\Delta U_0}{1+\exp[-\eta\Delta U_0 t - \Theta]}$$
$$U_{\text{mag}} = U_0^{\text{mag}} + \frac{\Delta U_0}{1+\exp[-\eta\Delta U_0 t - \Theta]} \tag{18}$$

where ΔU_0 is the initial energy difference between the two subsystems. The most important parameter of the logistic approach is the relaxation parameter η as it determines the time scales of the damping behavior for any excitations. The parameter Θ defines the inflection point. To verify the applicability of the logistic approach and to determine the two unknown parameters our simulation data for the internal energies of the lattice and the magnetization are fitted to Eq. (18). The result is shown in Fig. 4. The agreement of the logistic approach with the simulation data is remarkable. Only above the Curie temperature stronger deviations occur.

For better comparison to experimental data one can consider the relaxation rate, which can be calculated by

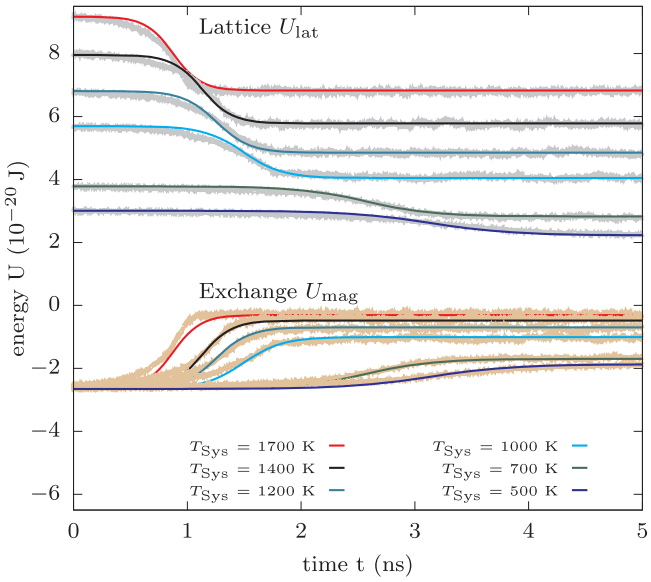

Fig. 4. Relaxation of an initially magnetically ordered cobalt cluster for different lattice temperatures. The agreement of the numerical data with the logistic model is remarkable. Only at very high temperature deviations occur.

$$\Gamma = \eta\Delta U_0, \tag{19}$$

as this rate can be obtained in ferromagnetic resonance measurements. Furthermore, theoretical modeling of the longitudinal ferromagnetic dynamics [45,46] in the high temperature regime assumes a linear dependence of spin-lattice relaxation. With our simulations we can confirm that the lattice dynamics can induce such behavior. As shown in FIG. 5 the linear increase of the relaxation rate is valid up to the Curie temperature. The relaxation rate increases by nearly an order of magnitude from room temperature up to the Curie temperature. This behavior can explain the increase of the magnetic damping for higher temperatures even in metals, as the electronic dissipative effects do not increase in the high temperature regime [16].

Interestingly, we also find that the relaxation dynamics strongly depends on the initial state of the spin system. To investigate this effect we compare in Fig. 6 the difference of the spin relaxation dynamics, varying the initial spin state between fully ordered and completely disordered. The magnetization after equilibration is in all simulations about $\mu_{\text{eq}}/\mu_s = 0.5$, so that in two cases the spin system relaxes towards a state with lower energy, while in the other cases it is excited.

For low initial magnetization the relaxation is nearly exponential, as the lattice can be considered as a heat sink for the spin system. The

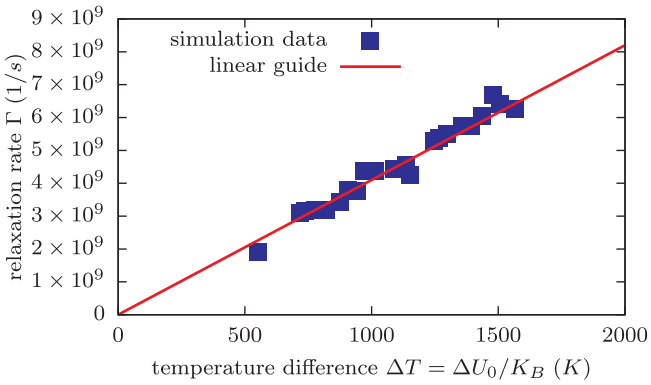

Fig. 5. Relaxation rates for different initial temperature differences of the both subsystems. The rates increase linearly up to the Curie temperature. This behavior is in good agreement with experimental findings. Again the results are obtained by fitting to temporal behavior of the inner energies depicted in Fig. 4.

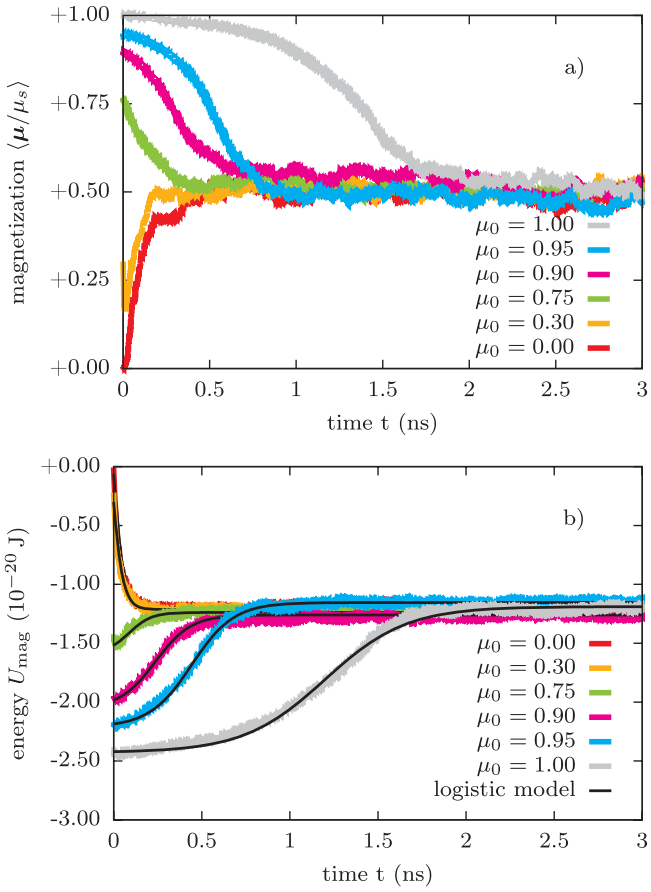

Fig. 6. Relaxation of the spin system of a cobalt cluster. Shown are in a) the magnetization and in b) the internal energy of the spin system. The initial conditions are varied from fully disordered to fully ordered but in equilibrium the magnetization is always about $\mu_{\mathrm{eq}}/\mu_s = 0.5$. We find a strong difference for the dynamics starting either above or below μ_{eq}.

logistic model can still be applied in this regime, but one is always behind the inflection point where the curve cannot be discriminated from an exponential decay. For initial magnetization above the equilibrium the spin system has to be excited from the coupling to the lattice and the logistic model fits well for the dynamics.

One can also see that the values of the parameters η and Θ depend on the initial magnetization and, with that, on the number of available magnons. With increasing initial number of magnons the parameter Θ (the inflection point) decreases, leading finally to a more exponential behavior. At the same time the damping effects become stronger with higher number of magnons available for scattering. To compare the resulting dissipation, we calculate the damping constant α in the LLG equation as

$$\alpha_{\mathrm{lat}} = \eta \mu_s / \gamma. \tag{20}$$

So α describes the dissipated energy per precession cycle of the magnetization. The damping parameters resulting from the obtained relaxation rates for low and high initial temperature of the magnetic system are calculated. For that two cases are considered. First when the magnetic system is completely ordered and therefore is at zero temperature and second then the magnetic system is at elevated temperature.

For Cobalt one calculates for low temperatures a value of $\alpha \approx 3 \times 10^{-5}$ and a value a magnitude larger for the high temperature regime $\alpha \approx 4 \times 10^{-4}$. For iron and nickel the values are almost the same for low temperatures (Fe: $\alpha \approx 3 \times 10^{-5}$, Ni: $\alpha \approx 2 \times 10^{-5}$), as well as in the elevated temperature regime (Fe: $\alpha \approx 8 \times 10^{-4}$, Ni: $\alpha \approx 2 \times 10^{-4}$). Comparing the resulting damping parameter values to the overall damping arising from electronic effects [16], one can see that the spin-lattice damping is at least one order of magnitude smaller. For the high temperature regime the gap closes, as the electronic effects become weaker [16] and the phononic effects stronger, but the electronic effects are still dominant. The linear increase of the damping constant for elevated lattice temperatures is in good agreement with experimental measurements [47]. Compared to the damping in magnetic insulators like YIG ($\alpha_{\mathrm{tot}} \approx 10^{-4}$–$10^{-6}$, see Ref. [20]) the resulting spin-lattice damping seems to be in a reasonable regime.

6. Summary

We suggest a model for combined simulations of spin and lattice degrees of freedom. The spin-lattice coupling obeys the conservation laws for energy and angular momentum and, hence, reproduced the Einstein-De Haas effect. We also suggest a possible parametrization of the model which rests on experimentally accessible data so that the approach can be applied to various materials. The spin system relaxation depends on initial state and can clearly deviate from a pure exponential behavior for fully saturated magnetization. In that case, the relaxation is better described by a logistic approach. We calculate the resulting relaxation rates, which are at least one order of magnitude smaller than the electronic dissipation effects in metals. However, in magnetic insulators like YIG this behavior could play a role for terahertz excitation as in this kind of experiment the phononic system can be strongly pumped.

Acknowledgment

We thank the Center for Applied Photonics at the University of Konstanz for financial support and Dr. Rocio Yanes-Diaz for fruitful discussions.

References

[1] E. Beaurepaire, J.-C. Merle, A. Daunois, J.-Y. Bigot, Ultrafast spin dynamics in ferromagnetic nickel, Phys. Rev. Lett. 76 (1996) 4250–4253.

[2] C. Stamm, T. Kachel, N. Pontius, R. Mitzner, T. Quast, K. Holldack, S. Khan, C. Lupulescu, E.F. Aziz, M. Wietstruk, H.A. Dürr, W. Eberhardt, Femtosecond modification of electron localization and transfer of angular momentum in nickel, Nat. Mater. 6 (10) (2007) 740.

[3] G. Malinowski, F. Dalla Longa, J.H.H. Rietjens, P.V. Paluskar, R. Huijink, H.J.M. Swagten, B. Koopmans, Control of speed and efficiency of ultrafast demagnetization by direct transfer of spin angular momentum, Nat. Phys. 4 (2008) 855.

[4] M. Battiato, K. Carva, P.M. Oppeneer, Theory of laser-induced ultrafast superdiffusive spin transport in layered heterostructures, Phys. Rev. B 86 (2012) 024404.

[5] B. Koopmans, G. Malinowski, F. Dalla Longa, D. Steiauf, M. Fähnle, T. Roth, M. Cinchetti, M. Aeschlimann, Explaining the paradoxical diversity of ultrafast laser-induced demagnetization, Nat. Mater. 9 (2009) 259.

[6] N. Kazantseva, U. Nowak, R.W. Chantrell, J. Hohlfeld, A. Rebei, Slow recovery of the magnetisation after a sub-picosecond heat pulse, EPL (Europhys. Lett.) 81 (2) (2008) 27004.

[7] U. Atxitia, O. Chubykalo-Fesenko, N. Kazantseva, D. Hinzke, U. Nowak, R.W. Chantrell, Micromagnetic modeling of laser-induced magnetization dynamics using the landau-lifshitz-bloch equation, Appl. Phys. Lett. 91 (23) (2007) 232507.

[8] F. Boschini, M. Mansurova, G. Mussler, J. Kampmeier, D. Grützmacher, L. Braun, F. Katmis, J.S. Moodera, C. Dallera, E. Carpene, C. Franz, M. Czerner, C. Heiliger, T. Kampfrath, M. Münzenberg, Coherent ultrafast spin-dynamics probed in three dimensional topological insulators, Sci. Rep. 5 (2015) 15304.

[9] K.W. Kim, M. Porer, A. Pashkin, A. Sell, T. Kampfrath, A. Leitenstorfer, and R. Huber. THz Spin Dynamics: Phonon-Induced Spin Order, volume 159, chapter Part IX, pages 327–330. Springer International Publishing, 2015.

[10] A.H. Reid, X. Shen, P. Maldonado, T. Chase, E. Jal, P. Granitzka, K. Carva, R.K. Li, J. Li, L. Wu, T. Vecchione, T. Liu, Z. Chen, D.J. Higley, N. Hartmann, R. Coffee, J. Wu, G.L. Dakowski, W. Schlotter, H. Ohldag, Y.K. Takahashi, V. Mehta, O. Hellwig, A. Fry, Y. Zhu, J. Cao, E.E. Fullerton, J. Stöhr, P.M. Oppeneer, X.J. Wang, and H.A. Dürr. Ultrafast spin-lattice coupling in laser-excited FePt nanoparticles. ArXiv e-prints, Feb 2016.

[11] G.E.W. Bauer, E. Saitoh, B.J. van Wees, Spin caloritronics, Nat Mater 11 (2012) 391.

[12] L. Landau, E. Lifshitz, On the theory of the dispersion of magnetic permeability in ferromagnetic bodies, Physik. Z. Sowjetunion 8 (1935) 153.

[13] T.L. Gilbert, A phenomenological theory of damping in ferromagnetic materials, IEEE Trans. Magn. 40 (2004) 3443.

[14] M. Fähnle, D. Steiauf, Dissipative magnetization dynamics close to the adiabatic regime, Handbook Magn. Adv. Magn. Mater. 1 (2007) 282.
[15] K. Gilmore, Y.U. Idzerda, M.D. Stiles, Identification of the Dominant Precession-Damping Mechanism in Fe Co, and Ni by First-Principles Calculations, Phys. Rev. Lett. 99 (2007) 027204.
[16] S. Mankovsky, D. Ködderitzsch, G. Woltersdorf, H. Ebert, First-principles calculation of the Gilbert damping parameter via the linear response formalism with application to magnetic transition metals and alloys, Phys. Rev. B 87 (2013) 014430.
[17] A.A. Starikov, P.J. Kelly, A. Brataas, Y. Tserkovnyak, G.E.W. Bauer, Unified first-principles study of gilbert damping, spin-flip diffusion, and resistivity in transition metal alloys, Phys. Rev. Lett. 105 (2010) 236601.
[18] A. Yu. Dobin, R.H. Victora, Intrinsic Nonlinear Ferromagnetic Relaxation in Thin Metallic Films, Phys. Rev. Lett. 90 (2003) 167203.
[19] H. Suhl, Theory of the magnetic damping constant, IEEE Trans. Magn. 34 (4) (1998) 1834–1838.
[20] G.A. Melkov, A.G. Gurevich, Magnetization Oscillation and Waves, CRC-Press, 1996.
[21] S. Karakurt, U. Nowak, R.W. Chantrell, A model of damping due to spin-lattice interaction, J. Magn. Magn. Mater. 316 (2007) 280.
[22] D. Perera, M. Eisenbach, D.M. Nicholson, G.M. Stocks, D.P. Landau, Reinventing atomistic magnetic simulations with spin-orbit coupling, Phys. Rev. B 93 (2016) 060402.
[23] C. Vittoria, S.D. Yoon, A. Widom, Relaxation mechanism for ordered magnetic materials, Phys. Rev. B 81 (2010) 014412.
[24] R.C. Le Craw, R.L. Comstock, Magnetoelastic interaction in ferromagnetic insulators, Phys. Acoust., Principles Methods 3 (1965) 127.
[25] A.I. Akhiezer, V.G. Bar'iakhtar, S.V. Peletminskii, Coupled magnetoelastic waves in ferromagnetic media and ferroacoustic resonance, JETP 8 (1) (1959) 157.
[26] A. Kamra, H. Keshtgar, P. Yan, G.E.W. Bauer, Coherent elastic excitation of spin waves, Phys. Rev. B 91 (2015) 104409.
[27] J.H. van Vleck, On the anisotropy of cubic ferromagnetic crystals, Phys. Rev. 52 (1937) 1178.
[28] C.H. Woo, Hai Wang, Pui-Wai Ma, Exchange interaction function for spin-lattice coupling in bcc iron, Phys. Rev. B 82 (2010) 144304.
[29] M. Pajda, J. Kudrnovský, I. Turek, V. Drchal, P. Bruno, Ab initio calculations of exchange interactions, spin-wave stiffness constants, and Curie temperatures of Fe Co, and Ni, Phys. Rev. B 64 (2001) 174402.
[30] M.A. Ruderman, C. Kittel, Indirect exchange coupling of nuclear magnetic moments by conduction electrons, Phys. Rev. 96 (1954) 99–102.
[31] T. Kasuya, A theory of metallic ferro- and antiferromagnetism on Zener's model, Progress Theoret. Phys. 16 (1) (1956) 45–57.
[32] K. Yosida, Magnetic properties of Cu-Mn alloys, Phys. Rev. 106 (1957) 893–898.
[33] D. Sander, The correlation between mechanical stress and magnetic anisotropy in ultrathin films, Rep. Prog. Phys. 62 (5) (1999) 809.
[34] N.W. Ashcroft, D.N. Mermin. Solid State Physics, volume 3A. Oldenbourg, 2007.
[35] Pui-Wai Ma, C.H. Woo, S.L. Dudarev, Large-scale simulation of the spin-lattice dynamics in ferromagnetic iron, Phys. Rev. B 78 (2008) 024434.
[36] P.J. Mohr, B.N. Taylor, D.B. Newell, CODATA recommended values of the fundamental physical constants: 2010*, Rev. Mod. Phys. 84 (2012) 1527–1605.
[37] D. Frenkel, B. Smit, Understanding Molecular Simulation vol. 2, Academic Press, 2002.
[38] M. Suzuki, Generalized Trotter's formula and systematic approximants of exponential operators and inner derivations with applications to many-body problems, Comm. Math. Phys 51 (2) (1976) 183–190.
[39] I.P. Omelyan, I.M. Mrygold, R. Folk, Algorithm for molecular dynamics simulation of spin liquids, Phys. Rev. Lett 86 (5) (2001) 898.
[40] J. Van Kranendonk, J.H. Van Vleck, Spin waves, Rev. Mod. Phys. 30 (1) (1958).
[41] A. Einstein, W.J. de Haas, Experimenteller Nachweis der Ampèreschen Molekularströme, Deutsche Physikalische Gesellschaft, Verhandlungen 17 (1915) 152.
[42] U. Nowak, Classical spin models, Handbook Magn. Adv. Magn. Mater. 1 (2) (2006) 858.
[43] A. Vaterlaus, T. Beutler, D. Guarisco, M. Lutz, F. Meier, Spin-lattice relaxation in ferromagnets studied by time-resolved spin-polarized photoemission, Phys. Rev. B 46 (1992) 5280–5286.
[44] K. Blum, Density Matrix Theory and Applications vol. 1, Plenum Press, New York, 1981.
[45] O. Chubykalo-Fesenko, U. Nowak, R.W. Chantrell, D. Garanin, Dynamic approach for micromagnetics close to the Curie temperature, Phys. Rev. B 74 (2006) 094436.
[46] D.A. Garanin, Fokker-Planck and Landau-Lifshitz-Bloch equations for classical ferromagnets, Phys. Rev. B 55 (1997) 3050.
[47] S.M. Bhagat, P. Lubitz, Temperature variation of ferromagnetic relaxation in the 3*d* transition metals, Phys. Rev. B 10 (1974) 179–185.